HHS Public Access
Author manuscript
Phys Chem Chem Phys. Author manuscript; available in PMC 2020 January 21.

Published in final edited form as:
Phys Chem Chem Phys. 2019 January 21; 21(3): 1254–1259. doi:10.1039/c8cp06299d.

Heavy Carbon Nanodots 2: Plasmon Amplification in Quanta Plate™ Wells and the Correlation with the Synchronous Scattering Spectrum

Rachael Knoblauch, **Estelle Ra**, and **Chris D. Geddes***
Institute of Fluorescence and Department of Chemistry and Biochemistry, University of Maryland, Baltimore County, 701 East Pratt Street, Baltimore, Maryland 21202, United States

Abstract

Brominated carbon nanodots are a new carbon nanostructure that exhibit strong phosphorescence without fixation. Herein we report plasmonic amplification of this phosphorescence in silver-coated Quanta Plate™ wells, a technique called Metal-Enhanced Phosphorescence (MEP). Subsequently we correlate the excitation and emission components of brominated carbon nanodots to their respective enhancement values. These properties are then discussed in relation to the synchronous scattering spectrum of the plasmonic substrate, in the first report of its kind for MEP. These results set the foundation for expanded application of carbon nanodots, as the photophysical characteristics of phosphorescence are improved, and augment the growing understanding of MEP.

Keywords

Metal-Enhanced Fluorescence; Metal-Enhanced Phosphorescence; quanta plate; plasmonic amplification; synchronous scattering spectrum; silver nanoparticles; nanotechnology; carbon nanodots; carbon dots

1.0. INTRODUCTION

Carbon nanodots have emerged over the past decade as a promising luminescent nanostructure for applications in fluorescence sensing and various biomedical fields.[1, 2] Phosphorescence from carbon nanodots, however, has not been explored until relatively recently.[3–6] In a previous publication, we reported the generation of new phosphorescent carbon nanodot structures termed “heavy carbon nanodots.”[7] Of these, brominated carbon nanodots under acidic conditions displayed easily detectable phosphorescent signals at room temperature with no additional fixation—being one of the first reported carbon nanodot structures to exhibit such strong phosphorescence at room temperature in liquid media.

*Corresponding Author. Tel: (410) 576-5723, Fax: (410) 576-5722, geddes@umbc.edu.

Author Contributions.
All information reported was written by Rachael Knoblauch and edited by Dr. Chris D. Geddes. All experiments were designed by and executed under the supervision of Dr. Chris D. Geddes and Rachael Knoblauch. Undergraduate researcher Estelle Ra aided in the implementation of experiments and collection of data.

Conflicts of Interest.
There are no conflicts of interest to declare.

Although the signal from these structures was notable, we were interested to see if the phosphorescence could be even further enhanced via plasmon amplification. Due to their long afterglow, phosphors are advantageous for use in off-gated detection methods for clearer signals devoid of biological autofluorescence; however, often times phosphorescence is low intensity and therefore impractical in application. Metal-Enhanced Fluorescence (MEF) is a well-known process by which the emissive intensity of fluorophores can be magnified when in proximity to metal nanoparticles.[8] Research by our lab has also shown this to also occur for phosphorescence (MEP), making low-yield phosphors brighter for expanded applications.[9–11] This is particularly significant for the development of luminescence-based biological assays; by having a strongly phosphorescent system, clear and sensitive detection of low-concentration species such as biomarkers and DNA may be permissible even in solutions that exhibit strong biological autofluorescence. The use of MEP rather than MEF platforms for assay development, therefore, could improve upon current technologies.[12, 13] Herein we report the plasmon amplification of fluorescence and phosphorescence from brominated carbon nanodots using commercially available silver Quanta Plate™ wells from URSA BioScience (www.ursabioscience.com). In addition, we examine photophysical trends that have been demonstrated previously for Metal-Enhanced Fluorescence; in particular, MEF studies have shown enhancement to be excitation *and* emission wavelength dependent, with the trends and magnitude of enhancement factors at each wavelength correlating to the synchronous scattering spectrum for the plasmonic material in question.[14–16] The synchronous scattering spectrum is collected when the source excitation wavelength and detected emission wavelength are equal ($\lambda_{ex} = \lambda_{em}$), and scanned over a particular wavelength range. As such, the resulting spectrum represents the material's ability to effectively scatter incident wavelengths, in particular for larger plasmonic nanoparticles where scattering—rather than absorption—dominates the extinction spectrum.[15, 17] By the radiating plasmon model of MEF, strength of enhancement is dependent upon these scattering properties, so correlation between the synchronous scattering spectrum and enhancement at different wavelengths is expected.[18] Although this has been demonstrated for MEF, this same phenomenon has *hitherto* not been investigated for MEP. We additionally note *spectral distortion* for enhanced phosphorescence from brominated carbon nanodots; red-edge distortion has been reported previously for MEF, but once again there have been no reports for MEP.[14, 19] The demonstration and characterization of MEP from brominated carbon nanodots herein sets the foundation for further tuning of plasmon-enhanced phosphorescence from carbon dots.

2.0. MATERIALS AND METHODS

2.1. Synthesis and sample preparation of carbon nanodot structures.

Brominated carbon nanodots (bromine dots) and carbon nanodots collected into water (water dots) were prepared through a combustion-based strategy as reported previously.[7] Samples were sonicated to re-disperse aggregates and subsequently were mixed with glycerol for a minimum of 24 hours before spectroscopic analysis. Acidic brominated carbon nanodots were neutralized with 5M sodium hydroxide (Fisher Scientific) prior to mixing. Rose Bengal (Sigma Aldrich) was used as a phosphorescent control and was absorption-matched at 532 nm to the bromine dots at 300 nm prior to mixing with glycerol.

2.2. Luminescence detection for carbon nanodot structures.

Cuvette measurements of fluorescence and phosphorescence for all samples were taken on a Horiba Scientific FluoroMax®−4P spectrofluorometer at room temperature. Phosphorescence was detected using an off-gated collection mode with the following parameters: flash count, 100; time per flash, 61 msec; flash delay, 0.05 msec; and sample window, 0.20 msec. Fluorescence, phosphorescence, and synchronous scattering ($\lambda_{ex} = \lambda_{em}$) spectra from samples in 96-well plates were collected using a Varian Cary Eclipse Florescence Spectrophotometer equipped with a plate reader. A sample volume of 200 μL was determined to be optimal for MEF and MEP detection (Fig. S1). Samples were cooled to approximately −10 °C and analysed. It is of note that phosphorescence is detectable both at −10 °C and at room temperature. Although this signal at room temperature was detectable using the Varian Cary Eclipse, the signal was not as strong as was detected using the FluoroMax®−4P. As such, the temperature was lowered to generate more favourable signal to noise ratios and improve detection. Spectral characteristics remain consistent for the tested structures at these temperatures. For phosphorescence collection using the Varian Cary Eclipse, the following parameters were used: decay time, 5 msec; number of flashes, 1; delay time, 0.1 msec; and gate time, 1.0 msec. Samples were analysed both in blank plates (Greiner Bio-One) and silvered wells (Quanta Plate™ 96-wells, URSA BioScience) as depicted in supplemental figure 2. Using an acidified solution of glycerol, it was confirmed that minimal to no Quanta Plate™ well degradation occurs over 40 minutes in a pH 1 environment (Fig. S3).

2.3. Calculations for percent signal enhancement from Quanta Plate™ wells.

A solution of water and glycerol was prepared to collect the plate baselines; subsequently these baseline values were subtracted from the sample spectra intensities at each wavelength to generate the “baseline subtracted” spectra. These were overlaid with spectra collected on the FluoroMax 4-P to ensure preserved spectral shape and were integrated over relevant wavelengths. The integrated percent enhancement ($\%_{Int}$) was calculated by the following equation:

$$\%_{Int} = \frac{\int_{\lambda_0}^{\lambda_f} \text{Emission, Quanta Plate}^{TM} - \int_{\lambda_0}^{\lambda_f} \text{Emission, Blank Plates}}{\int_{\lambda_0}^{\lambda_f} \text{Emission, Blank Plates}} \times 100 \quad (1)$$

Where λ_0 represents the shorter wavelength of the integration range and λ_f indicates the upper wavelength in this range. Baseline subtracted data was smoothed and fit after analysis, and *emission* wavelength dependent percent enhancements ($\%_{\lambda n}$) were calculated from the fitted data at each emission wavelength (λ_n) by equation 2:

$$\%_{\lambda n} = \frac{I_{\lambda n,\ \text{Quanta Plate}^{TM}} - I_{\lambda n,\ \text{Blank Plates}}}{I_{\lambda n,\ \text{Blank Plates}}} \times 100 \quad (2)$$

Where I is the emission intensity (a.u.) at wavelength n, which is an integer wavelength (nm) in the emission spectrum.

3.0. RESULTS AND DISCUSSION

3.1. Metal-Enhanced Fluorescence and Phosphorescence from Brominated Carbon Nanodots on Quanta Plate™ wells.

Bromine dots exhibit both fluorescence ($S_1 \rightarrow S_0$) and phosphorescence ($T_1 \rightarrow S_0$) emission when excited by ultraviolet (UV) wavelengths, as shown in Fig. 1. As reported previously, this triplet character of brominated carbon nanodots is also demonstrated in their fluorescence quantum yields and lifetimes. Water dots exhibit only fluorescence, with a quantum yield of ~10% and an average lifetime of 8.3 ns; however, we have shown that the fluorescence quantum yield and average lifetime of bromine dots drops to 4.9% and 6.2 ns respectively. Both of these changes correlate to the emergence of intersystem crossing as a competitive pathway to radiative S_1 emission, and in fact correspond to a detected long-lived lifetime of 92 μs, which is the phosphorescence lifetime of the brominated dots.[7] This dual emission from the S_1 and T_1 states, however, only occurs under acidic conditions for bromine dots. When neutralized (pH ~ 7), the bromine dots exclusively exhibit S_1 emission at room temperature, and in fact appear to regain some fluorescence intensity post pH adjustment in tandem with a loss of triplet emission.

This pH dependence of T_1 emission has been reported previously by our lab,[7] while pH dependence has also been reported for solely fluorescent carbon nanodots in numerous studies.[20–22] Acidic bromine dots display phosphorescence when excited at 300 nm, with the last detectable T_1 emission spectrum at approximately 350 nm. As such, we investigated the enhancement from each sample at 300, 325, and 350 nm excitation wavelengths. The emission of water dots is also included in this analysis to provide a non-phosphorescent structural analogue.

Metal-enhanced phosphorescence (MEP) from the acidic bromine dots in Quanta Plate™ wells was first investigated as depicted in Fig. 2.

As shown by the fitted data, the phosphorescence emission from the bromine dots was amplified by proximity to the nano-silver coating in the Quanta Plate™ wells. The signal detected at 350 nm excitation wavelength is of particular note, as the integrated intensity increased substantially as compared to the signal enhancement at 300 nm. Metal-Enhanced Fluorescence from the bromine dots was also investigated (Fig. 2). While enhancement was observed for fluorescence from bromine dots in both neutral and acidic conditions, large differences in shape between the blank and Quanta Plate™ well emission spectra—particularly at the blue edge and for longer excitation wavelengths—was noted. This is largely attributed to experimental parameters; because bromine dots are relatively low fluorescence emitters, larger slit widths were used to permit signal detection. Silver scatters incident light more strongly than the blank wells alone, altering the baseline and therefore distorting the calculated values. As such, the blue-edge wavelengths for which scattering was observed in the baseline spectra were not factored into the integrated percent enhancement calculations. We then compared the fluorescence enhancement of the bromine

dots to that of water dots prepared by the same combustion method (Fig. S4). Enhancement was also observed for the water dots albeit with minimal distortion of the integrated data on the blue edge due to baseline scattering, perhaps due to higher detected fluorescence intensity from the water dots alone, given an approximately 2-fold higher quantum yield.[7]

Although the irregular baselines inherent to fluorescence enhancement from bromine dots could make application of this technology challenging, it is interesting to note that this blue-edge spectral distortion for bromine dots is not observed for the phosphorescent emission for the same samples. This observation can be attributed to the decay rates of scattering, fluorescence, and phosphorescence. Scattering of light from the excitation source occurs on a similar time scale as fluorescence and is therefore detected alongside MEF under these experimental conditions. Conversely, phosphorescence occurs on a much longer time scale that requires an off-gated collection method, mentioned previously. Under these parameters, any residual excitation light has been elastically scattered by the beginning of signal collection and subsequently is not detected in the baseline for phosphorescence. Because phosphorescence signals are enhanced clearly and without background noise, a promising foundation is set for the development and application of MEP technologies using not only brominated carbon nanodots but also other low-intensity phosphors. Since the baseline is simplified by the off-gated collection method, calculations are more straightforward, and the entire emission spectrum can be considered for applications of MEP. To demonstrate the potential utility of Quanta Plate™ wells in the amplification of phosphorescence in general, we also tested Rose Bengal, a well-known phosphorescent compound, under the same sample preparation parameters used for the bromine dots (Fig. S5). Rose Bengal is a well-known phosphor and has been shown previously by our lab to demonstrate strong MEP.[11] Similar to bromine dots, the baseline detected from glycerol on blank and Quanta Plate™ wells is essentially negligible, with a clear enhancement observed.

Percent enhancements from Quanta Plate™ wells for all tested chromophores, pH values, and their respective emissions—including bromine dots ($T_1 \rightarrow S_0$ and $S_1 \rightarrow S_0$), Rose Bengal ($T_1 \rightarrow S_0$), and water dots ($S_1 \rightarrow S_0$)—are summarized in Table 1 and supplementary Figure S6.

From these collective data, it is evident that the fluorescence enhancement of acidic versus neutral bromine dots are comparable at each excitation wavelength. The phosphorescent signal from acidic bromine dots, however, demonstrates significantly higher enhancement relative to bromine dot fluorescence enhancements, and in fact achieves values comparable to those detected for Rose Bengal. Additionally, enhancement values for water dot fluorescence are similar in magnitude to those detected for phosphorescence from bromine dots. It is clear from these data that despite their nano-size and structural differences as compared to small molecular-sized fluorophores, carbon nanodot emission can be effectively plasmon amplified by silver Quanta Plate™ wells.

3.2. Correlation of photophysical properties to the synchronous scattering spectrum of silver.

We then questioned whether the enhancement from bromine dots under acidic conditions followed similar trends as were previously investigated and reported by our lab for other

fluorophores. In particular, MEF has been shown to exhibit *excitation* wavelength dependence that can be predicted by comparison to the synchronous scattering spectrum of the plasmonic material.[15] To date, however, this effect has not been tested for MEP. In Figure 3, integrated percent enhancements for bromine dot phosphorescence are plotted.

When plotted against excitation wavelength, the positive trend observed for bromine dot phosphorescence enhancement follows the positive change in scattering intensity from the silver Quanta Plate™ Wells. It is interesting to note, conversely, that the fluorescence enhancement from bromine dots does not correlate to the synchronous scattering spectrum closely, in particular at 350 nm excitation (Fig. 3b).

As mentioned previously, fluorophores have also been shown to demonstrate *emission* wavelength dependent enhancement,[14–16] so the integrated percent enhancements for bromine dot emission were plotted against λ_{max}. When plotted against peak emission wavelength, integrated percent enhancements of bromine dot *fluorescence* correlate closely to the trend and magnitude from the scattering spectrum for silvered wells (Fig. 3b). Integrated percent enhancements of phosphorescence, alternatively, do not exhibit a predictable correlation in magnitude (Fig. 3a). If one examines the general trend in scattering from silvered wells from 545 to 625 nm wavelengths (Fig. S7), however, it is clear that the overall trend in scattering is positive as incident wavelength is increased. This same positive trend is observed for the integrated percent enhancements of bromine dot *phosphorescence* (Fig. S7).

The statistical differences between integrated enhancements at 300, 325, and 350 nm excitation wavelengths were then analysed to confirm the significance of *excitation* wavelength dependence in carbon nanodot structures. A 2-tailed Student's T-test was performed, with the results presented in supplemental Figure S8. For MEF from bromine dots, both the acidic and neutral enhancements were averaged as no statistical difference was found between the values detected (Fig. S8a). Enhancement between 300 nm and 325 nm were found to be statistically different at a 98% confidence limit, whereas 300 nm vs 350 nm enhancements were found to be different with 95% confidence. No difference was found between enhancements for 325 and 350 nm excitation wavelengths. MEP from bromine dots also exhibits statistically significant differences between wavelengths, with the following confidence limits (%): 300 vs 325 nm, 95%; 300 vs 350 nm, 99.9%; 325 vs 350, 99% (Fig. S8b). Wavelength dependence for water dot fluorescence is also statistically significant with the following confidence limits: 300 vs 325 nm, 95%; 300 vs 350 nm, 99.8%; 325 vs 350 nm, 98% (Fig. S8c).

Previous studies into the mechanism of MEF have also shown enhancement to be *emission* wavelength dependent when excitation wavelength is held constant.[14–16] To determine if the bromine dots under various conditions demonstrate this dependence, the percent enhancements ($\%_{\lambda n}$) at each detected wavelength in the emission spectra were plotted (Fig. S9). Under neutral conditions, some dependence of MEF from bromine dots is observed, although this effect is more pronounced for fluorescence under acidic conditions. It is interesting to note that these trends follow the spectral shape of the synchronous scattering spectra from Quanta Plate™ wells containing either a neutral or acidic glycerol blank.

Although this effect is not well understood, current theory of MEF proposes two mechanisms of signal amplification: enhanced absorption and enhanced emission.[16] If enhancement is due to coupled emission from the excited fluorophore, then it would follow that this effect is more pronounced where the plasmonic material scatters light strongly. It is interesting to note, however, that this same correlation between emission dependent enhancement and synchronous scattering spectrum is not observed for *MEP* from bromine dots (Fig. S9c). In fact, excitation at 350 nm is the only experimental condition where percent enhancement ($\%_{\lambda n}$) at each emission wavelength correlates closely with the synchronous scattering spectrum. It is interesting to note that enhanced phosphorescence from Rose Bengal *does* exhibit emission wavelength dependence (Fig. S10), which stands in contrast to MEP from bromine dots. These trends reported for $\%_{\lambda n}$ for MEF and MEP from bromine dots in fact mimic those trends detailed previously for the *excitation* wavelength dependence of *integrated* percent enhancements ($\%_{int}$). Thus, MEF from bromine dots on silver can be predicted from the synchronous scattering spectra by examining emission wavelengths of interest, while excitation wavelength parameters are likely a more suitable predictor for the magnitude of MEP from bromine dots.

It is interesting to note that these observations are directly in line with the conclusions of a paper published by Geddes *et al* in 2013.[9] In that study, Geddes showed that the magnitude of enhanced phosphorescence and delayed fluorescence ($\alpha S_1 \rightarrow S_0$) closely followed the theoretical electric field decay around the plasmonic nanoparticles. Past literature has also reported experimental spectral distortion in plasmon-enhanced spectra of some fluorophores, in particular on the red edge.[14, 19] To determine if this effect was also present for MEP, the normalized spectra for Rose Bengal (Fig. S5b) and acidic bromine dots (Fig. S11) are compared. While Rose Bengal exhibits minimal if any variation in the spectral profile of the enhanced versus blank emission spectra, the bromine dots exhibit a sizable red-edge distortion. This effect becomes more pronounced at longer excitation wavelengths, although the mechanistic underpinning of this observation is *hitherto* little understood. Fluorophore lifetimes are also known to be impacted for MEF systems, as the inclusion of an additional radiative pathway from the coupled system will speed the excited decay rate.[23, 24] While this phenomenon, along with any potential quantum yield effects, would be beneficial to study using our MEF and MEP systems, the limitations of the experimental parameters described herein precluded this investigation. Further studies may elucidate these effects to deepen the understanding of the MEP mechanism.

4.0. CONCLUSIONS

Herein we have reported the plasmon amplification of brominated carbon nanodot emission by silver Quanta Plate™ wells. Our results demonstrate that both fluorescence and phosphorescence from these structures can be amplified, and that MEF can occur both under acidic and neutral conditions. Percent enhancement of fluorescence from bromine dots remains largely constant between samples of different pH excited under the same conditions, despite higher overall fluorescent intensity of bromine dots under neutral conditions. Metal-enhanced phosphorescence, however, is only observable under acidic conditions where this T_1 emission is detected without amplification. Nonetheless, percent enhancements of phosphorescence are in general higher and with less experimental noise as compared to the

enhanced fluorescence, establishing this MEP from bromine dots as potential route for improving the spectroscopic characteristics of phosphorescent carbon nanodot structures in the future. Strength of MEF from bromine dots was shown to be excitation wavelength dependent, with relative percent enhancements at each wavelength predictable based on peak emission wavelength of the blank emission spectra and the Quanta Plate™ well synchronous scattering spectrum. MEP efficiency was shown to also be excitation wavelength dependent, although in this case the relative enhancement better correlates to the synchronous scattering spectrum when plotted against excitation wavelength. MEF from bromine dots was also shown to be emission wavelength dependent, predictable at each wavelength based on the overall trends shown in the synchronous scattering spectrum. This same trend was not observed for MEP, except at 350 nm when the MEP effect is strongest. Interestingly, MEP from bromine dots exhibits red-edge spectral distortion akin to other reported fluorescence distortions for coupled MEF systems and is the first report of this distortion for MEP.

The research reported herein establishes plasmonic amplification of phosphorescence from brominated carbon nanodots as an intriguing new route for improving the brightness of these low-intensity phosphors. Through the use of commercially available silver Quanta Plate™ wells, clearer and stronger phosphorescent signals with improved signal to noise are detected from bromine dots at all relevant excitation wavelengths. These data set the foundation for further research into the optimization of MEP from bromine dots and present the opportunity for expanded applications of carbon nanodot structures in luminescence sensing.

Supplementary Material

Refer to Web version on PubMed Central for supplementary material.

ACKNOWLEGEMENT

The authors acknowledge the Institute of Fluorescence (IoF) as well as the Department of Chemistry and Biochemistry at the University of Maryland Baltimore County (UMBC) for financial support.

Funding Sources.

National Institutes of Health (NIH) Chemistry Biology Interface (CBI) Program at University of Maryland Baltimore County – 5T32GM066706-14.

Institute of Fluorescence at the University of Maryland Baltimore County Internal Funding.

ABBREIVATIONS

MEF	Metal-Enhanced Fluorescence
MEP	Metal-Enhanced Phosphorescence
BrCND	brominated carbon nanodots

REFERENCES

1. Hong GS, Diao SO, Antaris AL and Dai HJ, CHEMICAL REVIEWS, 2015, 115, 10816–10906. [PubMed: 25997028]

2. Namdari P, Negahdari B and Eatemadi A, Biomedicine & Pharmacotherapy, 2017, 87, 209–222. [PubMed: 28061404]
3. Kai J, Yuhui W, Congzhong C and Hengwei L, Chemistry of Materials, 2017, 29, 4866–4873.
4. He J, He Y, Chen Y, Zhang X, Hu C, Zhuang J, Lei B and Liu Y, CHEMICAL ENGINEERING JOURNAL, 2018, 347, 505–513.
5. Tao S, Lu S, Geng Y, Zhu S, Redfern SAT, Song Y, Feng T, Xu W and Yang B, Angewandte Chemie, 2018, 130, 2417–2422.
6. Li Q, Zhou M, Yang M, Yang Q, Zhang Z and Shi J, Nature Communications, 2018, 9, 734–734.
7. Knoblauch R, Bui B, Raza A and Geddes CD, Physical Chemistry Chemical Physics: PCCP, 2018, 20, 15518–15527. [PubMed: 29808871]
8. Geddes CD, Metal-enhanced fluorescence, Hoboken, N.J. : Wiley, c2010, 2010.
9. Mishra H, Mali BL, Karolin J, Dragan AI and Geddes CD, Phys. Chem. Chem. Phys, 2013, 15, 19538–19544. [PubMed: 24100377]
10. Yongxia Z, Aslan K, Previte MJR, Malyn SN and Geddes CD, Journal of Physical Chemistry B, 2006, 110, 25108–25114.
11. Zhang Y, Aslan K, Malyn SN and Geddes CD, Chemical Physics Letters, 2006, 427, 432–437.
12. Dragan AI, Albrecht MT, Pavlovic R, Keane-Myers AM and Geddes CD, Analytical Biochemistry, 2012, 425, 54–61. [PubMed: 22406431]
13. Jeong Y, Kook Y-M, Lee K and Koh W-G, Biosensors and Bioelectronics, 2018, 111, 102–116. [PubMed: 29660581]
14. Ben Hamo H, Kushmaro A, Marks R, Karolin J, Mali B and Geddes CD, APPLIED PHYSICS LETTERS, 2015, 106.
15. Dragan AI, Mali B and Geddes CD, Chemical Physics Letters, 2013, 556, 168–172.
16. Geddes CD, JOURNAL OF PHYSICAL CHEMISTRY C, 2009, 113, 12095–12100.
17. Aslan K and Geddes CD, JOURNAL OF PHYSICAL CHEMISTRY C, 2008, 112, 18368–18375.
18. Aslan K, Leonenko Z, Lakowicz JR and Geddes CD, Journal of Fluorescence, 2005, 15, 643. [PubMed: 16341780]
19. Geddes CD, APPLIED PHYSICS LETTERS, 2014, 105.
20. Li H, Ming H, Liu Y, Yu H, He X, Huang H, Pan K, Kang Z and Lee ST, Journal, 2011, 2666.
21. Xu Z-Q, Lan J-Y, Jin J-C, Gao T, Pan L-L, Jiang F-L and Liu Y, Colloids and Surfaces B: Biointerfaces, 2015, 130, 207–214. [PubMed: 25910636]
22. Xu H, Yan L, Nguyen V, Yu Y and Xu Y, Applied Surface Science, 2017, 414, 238–243.
23. Karolin JO and Geddes CD, JOURNAL OF FLUORESCENCE, 2012, 22, 1659–1662. [PubMed: 23054299]
24. Yongxia Z, Dragan A and Geddes CD, Journal of Physical Chemistry C, 2009, 113, 15811–15816.

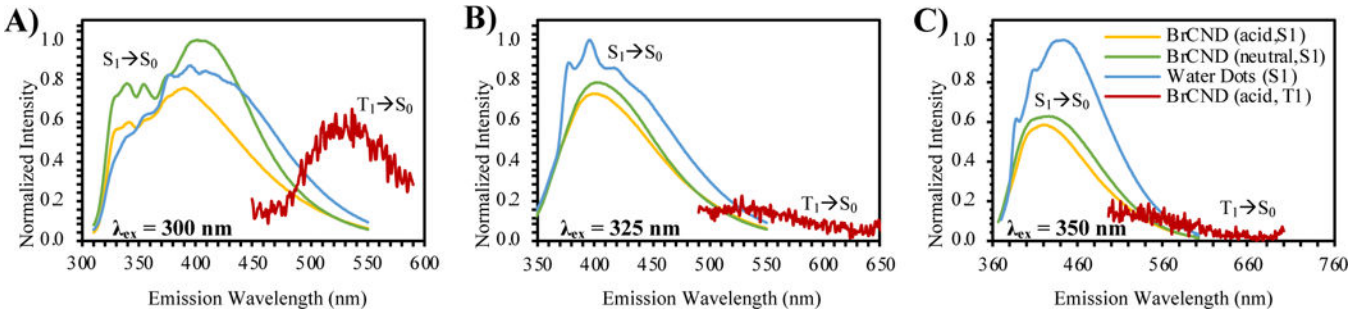

Fig 1.

Emission (normalized relative to overall intensity maximum for each excitation wavelength) of both fluorescence ($S_1 \rightarrow S_0$) and phosphorescence ($T_1 \rightarrow S_0$), from brominated carbon nanodots and water dots when excited at *A)* 300 nm, *B)* 325 nm, and *C)* 350 nm. (BrCND: brominated carbon nanodots)

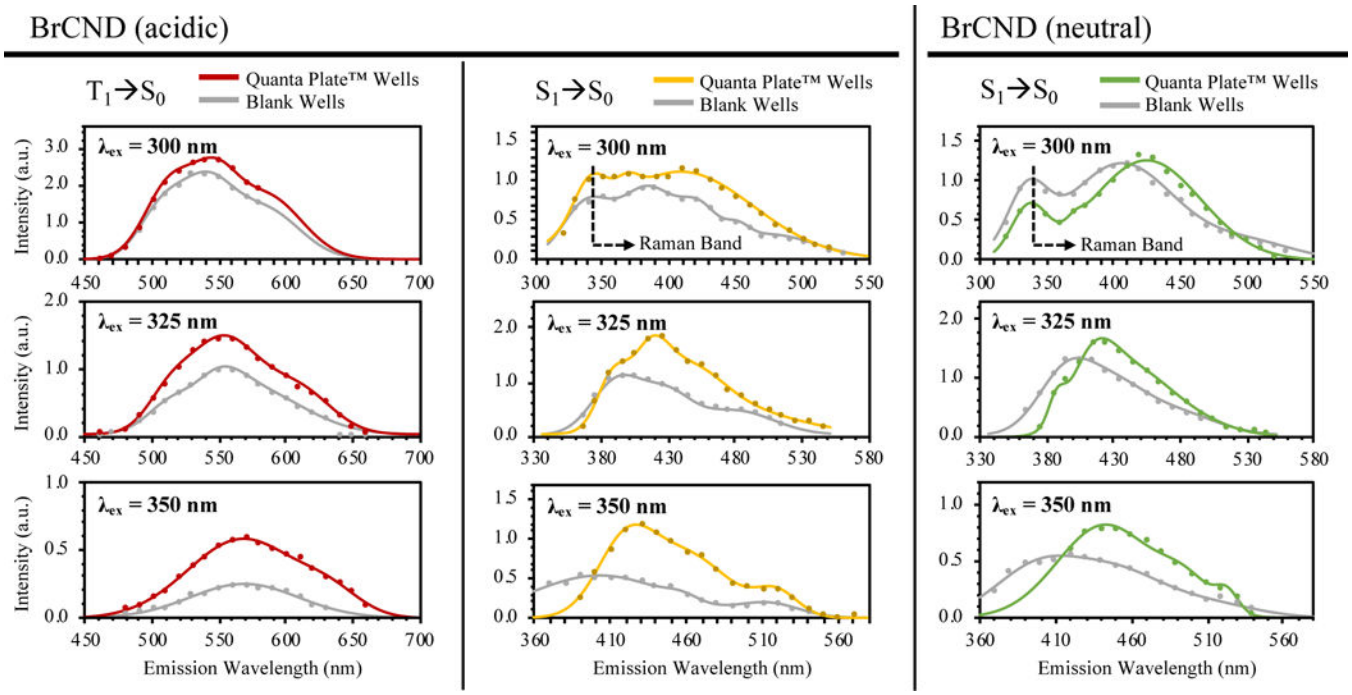

Fig. 2.

Fits (solid line) and smoothed raw data (dots) of enhanced phosphorescence (MEP, $T_1 \rightarrow S_0$) and fluorescence (MEF, $S_1 \rightarrow S_0$) emission from brominated carbon nanodots, mixed in glycerol, in silver Quanta Plate™ wells. Temperature at 0 to −10 °C, excited at wavelengths of 300 nm (integration ranges – MEP: 450–580 nm, MEF: 420–550 nm), 325 nm (integration ranges – MEP: 450–630 nm, MEF: 415–550 nm), and 350 nm (integration ranges – MEP: 450–650 nm, MEF: 445–600 nm).

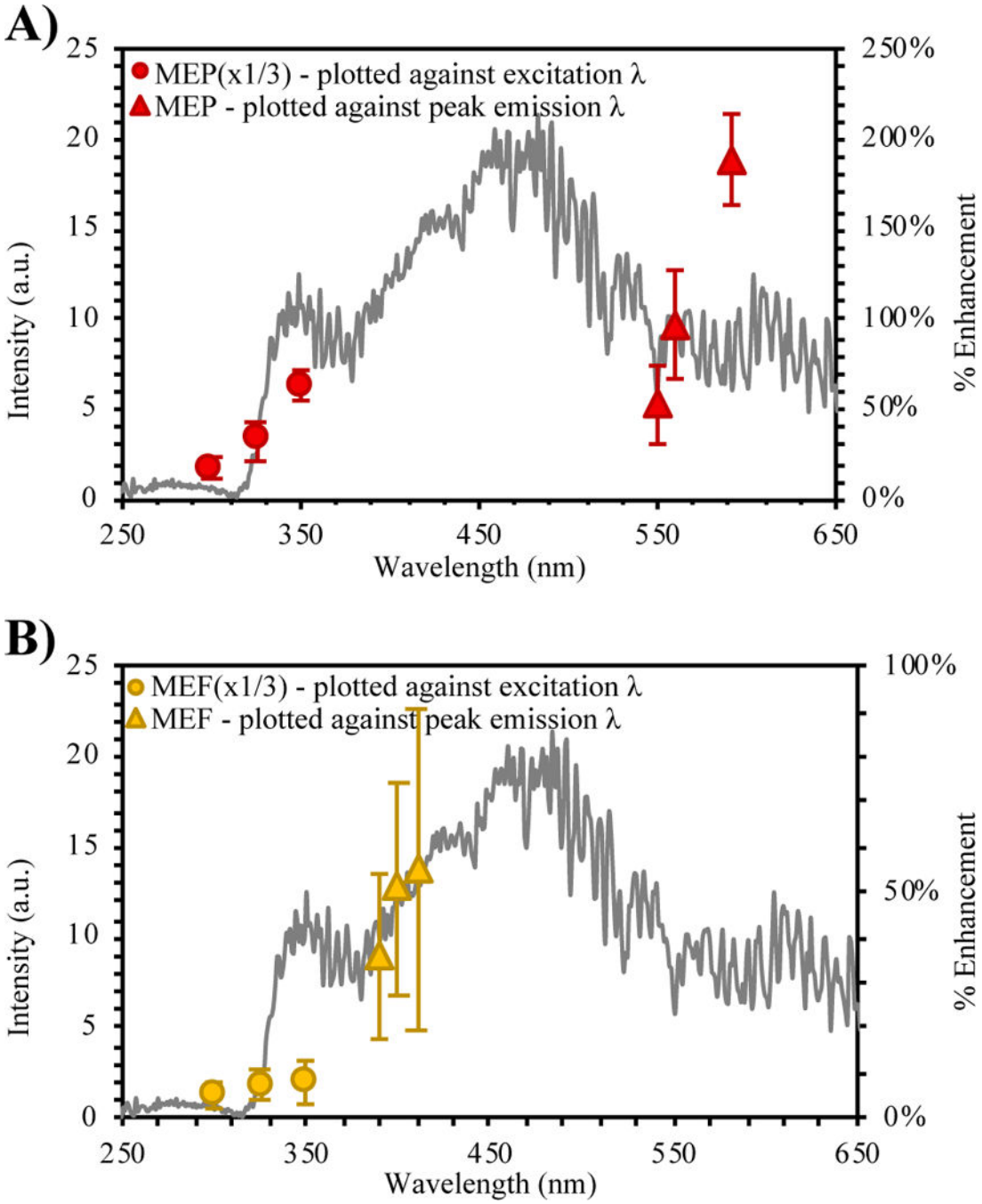

Figure 3.

Integrated percent enhancement for brominated carbon nanodots (acidic, glycerol) overlaid on synchronous scattering spectrum for Quanta Plate™ wells containing acidified glycerol. *A)* Metal-enhanced phosphorescence (MEP). *B)* Metal-Enhanced Fluorescence (MEF).

Table 1.

Percent Enhancement Values for Carbon Nanodots and Controls on Quanta Plate™ Wells.

Sample	λ_{ex} (nm)	Percent Enhancement (%)
BrCND (acidic)-MEP	300	50 ± 20
	325	100 ± 30
	350	190 ± 30
BrCND (acidic)-MEF	300	40 ± 20
	325	50 ± 30
	350	60 ± 30
BrCND (neutral)-MEF	300	20 ± 20
	325	50 ± 20
	350	70 ± 50
Water dots-MEF	300	45 ± 5
	325	100 ± 20
	350	160 ± 10
Rose Bengal-MEP	532	110 ± 20

λ_{ex} – excitation wavelength